frontiers in Marine Science

ORIGINAL RESEARCH
published: 31 March 2021
doi: 10.3389/fmars.2021.655714

Sodium-Dependent Phosphate Transporter Protein 1 Is Involved in the Active Uptake of Inorganic Phosphate in Nephrocytes of the Kidney and the Translocation of P_i Into the Tubular Epithelial Cells in the Outer Mantle of the Giant Clam, *Tridacna squamosa*

Yuen K. Ip[1], Mel V. Boo[1], Jeslyn S. T. Poo[1], Wai P. Wong[1] and Shit F. Chew[2]*

[1] Department of Biological Sciences, National University of Singapore, Singapore, Singapore, [2] Natural Sciences and Science Education, National Institute of Education, Nanyang Technological University, Singapore, Singapore

OPEN ACCESS

Edited by:
Youji Wang,
Shanghai Ocean University, China

Reviewed by:
Zhang Yuehuan,
South China Sea Institute of Oceanology (CAS), China
Maria Giulia Lionetto,
University of Salento, Italy

***Correspondence:**
Yuen K. Ip
dbsipyk@nus.edu.sg
orcid.org/0000-0001-9124-7911

Specialty section:
This article was submitted to Aquatic Physiology, a section of the journal Frontiers in Marine Science

Received: 19 January 2021
Accepted: 12 March 2021
Published: 31 March 2021

Citation:
Ip YK, Boo MV, Poo JST, Wong WP and Chew SF (2021) Sodium-Dependent Phosphate Transporter Protein 1 Is Involved in the Active Uptake of Inorganic Phosphate in Nephrocytes of the Kidney and the Translocation of P_i Into the Tubular Epithelial Cells in the Outer Mantle of the Giant Clam, Tridacna squamosa. Front. Mar. Sci. 8:655714. doi: 10.3389/fmars.2021.655714

Giant clams display light-enhanced inorganic phosphate (P_i) absorption, but how the absorbed P_i is translocated to the symbiotic dinoflagellates living extracellularly in a tubular system is unknown. They can accumulate P_i in the kidney, but the transport mechanism remains enigmatic. This study aimed to elucidate the possible functions of sodium-dependent phosphate transporter protein 1-homolog (PiT1-like), which co-transport Na^+ and $H_2PO_4^-$, in these two processes. The complete cDNA coding sequence of *PiT1-like*, which comprised 1,665 bp and encoded 553 amino acids (59.3 kDa), was obtained from the fluted giant clam, *Tridacna squamosa*. In the kidney, PiT1-like was localized in the plasma membrane of nephrocytes, and could therefore absorb P_i from the hemolymph. As the gene and protein expression levels of PiT1-like were up-regulated in the kidney during illumination, PiT1-like could probably increase the removal of P_i from the hemolymph during light-enhanced P_i uptake. In the ctenidial epithelial cells, PiT1-like had a basolateral localization and its expression was also light-dependent. It might function in P_i sensing and the absorption of P_i from the hemolymph when P_i was limiting. In the outer mantle, PiT1-like was localized in the basolateral membrane of epithelial cells forming the tertiary tubules. It displayed light-enhanced expression levels, indicating that the host could increase the translocation of P_i from the hemolymph into the tubular epithelial cells and subsequently into the luminal fluid to support increased P_i metabolism in the photosynthesizing dinoflagellates. Taken together, the accumulation of P_i in the kidney of giant clams might be unrelated to limiting the availability of P_i to the symbionts to regulate their population.

Keywords: photosynthesis, shell formation, Symbiodiniaceae, symbiosis, zooxanthellae

INTRODUCTION

Tropical waters are low in nutrients, but coral reefs, which are hubs of a wide variety of marine organisms including scleractinian corals and giant clams, can be found in shallow tropical waters with adequate irradiance. Specifically, giant clams (genus: *Tridacna* or *Hippopus*) are inhabitants of the Indo-Pacific reef ecosystems. They can grow rapidly despite the shortage of nutrients and are the largest of all bivalves, because they live in symbiosis with mainly three genera (*Symbiodinium*, *Cladocopium*, and *Durusdinium*; LaJeunesse et al., 2018) of phototrophic dinoflagellates belonging to the family Symbiodiniaceae (Hernawan, 2008; Weber, 2009; DeBoer et al., 2012; Ikeda et al., 2017; Lim et al., 2019). In giant clams, symbiotic dinoflagellates (zooxanthellae) reside extracellularly in a branched tubular system that originates from the digestive tract of the host (Norton and Jones, 1992). They are located mainly inside numerous tertiary tubules in the colorful and extensible outer mantle that contains pigments and iridocytes (Norton and Jones, 1992). During insolation, the outer mantle can be fully extended, and the host iridocytes can deflect light of appropriate wavelengths to the dinoflagellates to promote photosynthesis. Photosynthesizing dinoflagellates can donate as much as 95% of photosynthates to the host clam to fulfill its energy and nutrition requirements (Klumpp and Griffiths, 1994). In turn, the host must provide the symbionts with nutrients such as inorganic carbon (C_i), nitrogen (N), and phosphorous (P), because they have no access to the ambient seawater (Furla et al., 2005). As a consequence, the clam host displays many light-dependent physiological phenomena (Ip et al., 2006, 2015; see Ip and Chew, 2021 for a review), including light-enhanced uptake of C_i (Hiong et al., 2017a; Ip et al., 2018; Koh et al., 2018; Chew et al., 2019), N (Hiong et al., 2017b; Chan et al., 2018, 2019; Ip et al., 2020), and P (Chan et al., 2020). P is one of the essential elements for living systems, and inorganic phosphate (P_i) is needed for syntheses of ATP, phospholipids and genetic materials (Knowles, 1980), as well as for intracellular signaling (Olsen et al., 2006). Dissolved P_i comprises dihydrogen phosphate ($H_2PO_4^-$), hydrogen phosphate (HPO_4^{2-}), and phosphate (PO_4^{3-}), with HPO_4^{2-} and $H_2PO_4^-$ being the major components in water at pH 7.

Despite being deprived of access to planktonic/particulate matter, the fluted giant clam, *T. squamosa*, can survive and grow in Millipore-filtered seawater for more than 10 months with light as the sole energy source (Fitt and Trench, 1981). Without feeding, the clam host needs to receive adequate supplies of energy and nutrients from its phototrophic symbionts (Klumpp and Griffiths, 1994) in order to grow and conduct light-enhanced calcification. As symbionts are P-deficient, the host must supply them with P_i, which is absorbed from the ambient seawater, through the hemolymph and tubular fluid (Jackson et al., 1989). Although the concentration of P_i in seawater is low (0.08–0.50 μmol l^{-1}; Rivkin and Swift, 1985; Godinot et al., 2009), *T. squamosa* can absorb exogenous P_i, and the rate of P_i absorption is higher in light than in darkness (Chan et al., 2020; Ip and Chew, 2021). *T. squamosa* expresses a homolog of sodium-dependent phosphate transport protein 2a (NPT2a-like) in the apical membranes of the epithelia of three organs (Chan et al., 2020). These include the upper epithelium of the colorful outer mantle, the seawater-facing epithelium of the whitish inner mantle, and the epithelium covering the ctenidial filaments. Hence, the apical NPT2a-like in these epithelia can participate in P_i absorption from the ambient seawater. In addition, the protein abundance of NPT2a-like in the outer mantle, but not those in the other two organs, is up-regulated by illumination, denoting the outer mantle as a crucial site of light-enhanced P_i absorption (Chan et al., 2020). It is probable that the host could deliver the P_i absorbed through the outer mantle epithelium directly to symbionts residing therein, and regulate the supply of P_i absorption partially through NPT2a-like. As such, the photosynthesizing symbionts are spared from competing with other host's organs for the limiting P_i available in the hemolymph (Chan et al., 2020). In particular, the kidneys of giant clams are known to absorb and accumulate P_i, although the transporter involved remains unknown (Belda and Yellowlees, 1995).

It has been reported that the intracellular P_i concentration and the rate of division in cultured dinoflagellates isolated from *Tridacna gigas* increase after exposure to 10 μmol l^{-1} P_i. By contrast, the density of dinoflagellates and their N:P ratio remain unchanged in *T. gigas* exposed to 10 μmol l^{-1} P_i (Belda and Yellowlees, 1995). Therefore, it has been suggested that the host clam could absorb and store P_i in the kidney, thereby controlling the availability of P_i to the symbionts so as to regulate their population (Belda and Yellowlees, 1995). However, the kidney of *T. squamosa* has only weak expression of *NPT2a-like*, leading Chan et al. (2020) to postulate that other types of phosphate transporter could be present in the host's kidney tissues and the epithelium of the host's zooxanthellal tubules (Chan et al., 2020).

Phosphate transporters are members of the solute carrier family of proteins (SLC), and they consist of SLC17 (Type I), SLC34 (Type II), and SLC20 (Type III) (Virkki et al., 2007). Members of SLC20 and SLC34 are involved in the secondary active uptake of P_i in cells (Virkki et al., 2007; Forster et al., 2013). NPT2s are members of SLC34 that bind to HPO_4^{2-} and transport it together with Na^+ (Virkki et al., 2007). On the other hand, SLC20 consists of sodium-dependent phosphate transport proteins (PiTs; Forster et al., 2013) that co-transport Na^+ and $H_2PO_4^-$ (Virkki et al., 2007). PiTs are regarded as house-keeping transporters involved in phosphate metabolism in mammals, and it consists of sodium-dependent phosphate transporter protein 1 (PiT1) (SLC20A1) and PiT2 (SLC20A2) (Forster et al., 2013). In mammals, PiT1 is vital in embryonic liver development and in bone metabolism, while PiT2 has a more specific role in phosphate homeostasis in the brain (Forster et al., 2013). Furthermore, PiT1 and PiT2 can function as P_i sensing and signaling mechanisms by binding with external P_i but without translocation (Bon et al., 2017).

The populations of giant clams have been decreasing due to combinations of overharvesting for food and aquarium trade, pollution, and anthropogenic activities (Watson, 2015). Particularly, a decrease in the internal population of symbiotic dinoflagellates in giant clams can occur due to increased ocean temperature resulting from global warming (Addessi, 2001).

As the symbiont population could be controlled by the P_i concentration in the tubular fluid, it is essential to understand the molecular mechanisms of P_i transport in the host's kidney and those tissues that are involved in the supply of P_i to the symbionts. Therefore, this study was undertaken to clone and sequence a homolog of *PiT1* (*PiT1-like*) of host origin from the kidney of *T. squamosa*. Efforts were made to examine the gene expression of *PiT1-like* in various organs of *T. squamosa* to test the hypothesis that it was expressed predominantly in the kidney. Subsequently, we discovered that *PiT1-like* was also expressed strongly in the ctenidium and moderately in the outer mantle. Hence, in order to elucidate the cellular and subcellular localization of PiT1-like in the kidney, ctenidium and outer mantle, an anti-PiT1-like polyclonal antibody was custom-made to perform immunofluorescence microscopy. Furthermore, quantitative real-time PCR (qPCR) and western blotting were performed to determine the effects of light exposure on the transcript levels and protein abundances of *PiT1-like*/PiT1-like in these three organs of *T. squamosa.*

MATERIALS AND METHODS

Experimental Animals, Conditions, and Tissue Collection

Individuals of *T. squamosa* specimens (520 ± 180 g with shells; n = 19) were purchased from Xanh Tuoi Tropical Fish Ltd., in Vietnam. They were acclimated in three glass tanks (L90 cm × W62 cm × H60 cm) under a 12 h light:12 h dark regime for one month before experimentation. Each tank contained 350 L of recirculating seawater and 6 or 7 clams. The water conditions were as follows: salinity, 30–32; temperature, ∼26°C; pH, 8.1–8.3; hardness, 143–179 ppm; calcium, 380–420 ppm; phosphate, <0.25 ppm; nitrate, 0 ppm; nitrite, 0 ppm; total ammonia, <0.25 ppm. The underwater light intensity (PPFD) at the level of the clam was ∼120 μmol m^{-2} s^{-1}.

Four individuals (controls; n = 4) were sampled directly and randomly from all the three glass tanks, and killed for tissue sampling after 12 h of darkness in the normal 12 h light:12 h dark regime. Other individuals were then exposed to light for 3, 6, or 12 h. At each specific time points, four individuals (n = 4) were randomly selected and killed for tissue sampling. Individual clams were anesthetized with 0.2% phenoxyethanol before being forced open to cut the adductor muscles. Collected tissue samples were stored at −80°C until analyses.

After being anesthetized in 0.2% phenoxyethanol, three individuals exposed to darkness for 12 h (n = 3) were killed for the sampling of tissues for immunofluorescence microscopy. Samples were immersion-fixed in 3% paraformaldehyde in seawater at 4°C overnight and processed according to the method of Hiong et al. (2017a).

Extraction of Total RNA and Synthesis of cDNA

The total RNA from tissue samples was isolated using TRI Reagent™ (Sigma-Aldrich Co. St. Louis, MO, United States). Samples were homogenized with silica beads (425–600 μm; Sigma-Aldrich) in TRI Reagent® using a Mini-G™ tissue homogenizer (SPEX® Sample Prep, Metuchen, NJ, United States). Remnant of DNA was removed by PureLink™ RNA Mini Kit (Invitrogen, Thermo Fisher Scientific Inc., Waltham, MA, United States), and the purified RNA was quantified by a Shimadzu BioSpec-nano spectrophotometer (Shimadzu Corporation, Tokyo, Japan). After verification of the integrity of RNA by electrophoresis, cDNA was synthesized from the purified total RNA using the RevertAid™ first-strand cDNA synthesis kit (Thermo Fisher Scientific Inc.).

PCR, Cloning, Rapid Amplification of cDNA Ends (RACE)-PCR and Sequencing

A partial *PiT1-like* sequence was isolated using a pair of PCR primers (forward: 5′-TGATCGTTGGTTCCTGGTT-3′; reverse: 5′-TCGCCAATCGTATTGATGAC-3′) designed from the conserved regions of the sodium-dependent phosphate transporter 1 of *Octopus vulgaris* (XM_029794590.1), *Crassostrea gigas* (XM_020063507.2), *Crassostrea virginica* (XM_022469514.1), *Mizuhopecten yessoensis* (XM_021500463.1), and *Priapulus caudatus* (XM_014826122.1). The PCR was conducted using a 9902 Veriti 96-well thermal cycler (Applied Biosystems, Carlsbad, CA, United States) and DreamTaq™ polymerase (Thermo Fisher Scientific Inc.). The thermal cycling conditions included an initial denaturation at 95°C held for 3 min, followed by 40 cycles of denaturation, annealing and extension at 95°C for 30 s, 55°C for 30 s, and 72°C for 1 min, respectively, and a final extension for 10 min at 72°C. Agarose gel electrophoresis was used to separate the PCR products, and the Wizard® SV Gel and PCR clean-up system (Promega Corporation, Madison, WI, United States) was used to extract the targeted bands.

Following the method of Chan et al. (2020), the pGEM-T Easy vector system (Promega Corporation) was used to clone and transform the extracted PCR product into JM109 *Escherichia coli* competent cells. Multiple clones of *PiT1-like* were sequenced bi-directionally. BlastN[1] was used to confirm the identity of the sequences obtained. Analysis of multiple sequences revealed the absence of isoforms. The full coding sequence of *PiT1-like* was obtained by conducting 5′ and 3′ RACE-PCR (SMARTer™ RACE cDNA amplification kit; Clontech Laboratories, Mountain View, CA, United States) with specific RACE primers (forward: 5′-TTCCTGCAAATCCTTACTGCTGTGTT-3′, reverse: 5′-CAA TTCGGATCCTTTGTAGAAGACAG-3′).

BigDye Terminator v3.1 Cycle Sequencing Kit (Thermo Fisher Scientific Inc.) was used to prepare samples for sequencing, and sequencing was performed using a 3130XL Genetic Analyzer (Thermo Fisher Scientific Inc.). Sequences obtained were assembled and analyzed using BioEdit version 7.2.5. The GenBank Accession number of the full coding sequence of *PiT1-like* obtained from *T. squamosa* is MN256447.

[1]http://www.ncbi.nlm.nih.gov/BLAST

Deduced Amino Acid Sequence

The nucleotide sequence was translated into PiT1-like amino acid sequence using the ExPASy Proteomic server[2]. The deduced amino acid sequence was aligned with selected PiT1-like sequences from various species of mollusks and vertebrates to confirm its identity. The TOPCONS server was used to predict the transmembrane regions (TMs).

Gene Expression of PiT1-Like in Various Organs of *T. squamosa* and Quantification of Transcript Levels of PiT1-Like From the Kidney and Outer Mantle by qPCR

The gene expression of *PiT1-like* in the outer mantle, inner mantle, ctenidium, kidney, heart, hepatopancreas, adductor muscle, byssal retractor muscle, and foot muscle of *T. squamosa* was examined quantitatively by qPCR with gene-specific qPCR primers (forward: 5′-CAATCCTGGTTCGTCTGCTG-3′; reverse: 5′-TCTCAACAAGAACTCCCTCCTC-3′). qPCR was carried out with a StepOnePlus™ Real-Time PCR System (Thermo Fisher Scientific) and each reaction contained various quantities of cDNA of sample, 0.3 μmol l^{-1} each of specific forward and reverse primers and 5 μl of qPCRBIO SyGreen Mix (PCR Biosystems Ltd., London, United Kingdom). The cycling conditions consisted of an initial 20 s denaturation and enzyme activation at 95°C, 40 cycles of 95°C for 3 s and 60°C for 30 s. Absolute quantification of transcript level of *PiT1-like* from the kidney, ctenidum, and outer mantle were performed in triplicates. The specific qPCR primers had a amplification efficiency of 93%. The transcript level in the sample was estimated using a standard curve constructed according to the method of Hiong et al. (2017a).

Antibodies

For immunofluorescence microscopy and western blotting, a commercial firm (GenScript, Piscataway, NJ, United States) was engaged to produce a custom-made rabbit polyclonal anti-PiT1-like antibody against the epitope TPSSGFSIEVGSAA (residue 468–481) of PiT1-like of *T. squamosa*. For western blotting, an anti-α-tubulin antibody, 12G10 (Developmental Studies Hybridoma Bank, Department of Biological Sciences, University of Iowa, Iowa City, IA, United States), was used to detect the reference protein, α-tubulin.

Western Blotting

Proteins were extracted from samples of kidney, ctenidium, and outer mantle following the method of Hiong et al. (2017a). SDS-PAGE (10%) electrophoresis was applied to separate proteins of kidney (20 μg), ctenidium (50 μg) or outer mantle (100 μg) samples. Separated proteins were blotted onto a nitrocellulose membrane, which was then incubated for 1 h at 25°C with anti-PiT1-like (2 μg ml^{-1}) or anti-α-tubulin (12G10, 0.05 μg ml^{-1}) antibody. The membrane was processed using the Pierce Fast Western Blot kit, SuperSignal® West Pico Substrate (Thermo Fisher Scientific Inc.). Visualization of protein bands was achieved using a ChemiDoc™ MP Imaging System (Bio-Rad Laboratories Inc., Hercules, CA, Untied States). Optical density of the protein bands were determined using ImageJ (version 1.50i, NIH) and a 21-step Tiffen (The Tiffen Company, Rochester, NY, Untied States) transmission photographic step tablet (EK1523406T). Protein abundance of PiT1-like was expressed as the optical density of the PiT1-like band normalized with that of the α-tubulin band. As the protein expression level of PiT1-like was the highest in kidney, a peptide competition assay (PCA) was performed to validate the specificity of the custom-made anti PiT1-like antibody on kidney exposed to light for 12 h (**Supplementary Figure 1**). The anti-PiT1-like antibody was incubated with neutralizing peptide (Genscript) in a ratio of 1:5 for 1 h prior to western blotting.

Immunofluorescence Microscopy

Samples of the kidney, ctenidium, and outer mantle were excised and immersion-fixed overnight in 3% paraformaldehyde in seawater at 4°C, and processed according to the method of Hiong et al. (2017b). The paraffin-embedded samples were sectioned (3 μm) using a Leitz 1512 rotary microtome (Leica Biosystems, Germany) and collected on slides. Antigen retrieval was performed by treating deparaffinized sections with heated solution of 0.05% citraconic anhydride (Nacalai Tesque, Japan), pH 7.4, for 5 min with a further 10 min incubation in 1% sodium dodecyl sulfate (SDS) solution at room temperature. The section was blocked in 1% BSA in TPBS (0.05% Tween-20 in phosphate-buffered saline: 10 mmol l^{-1} Na_2HPO_4, 1.8 mmol l^{-1} KH_2PO_4, 137 mmol l^{-1} NaCl, 2.7 mmol l^{-1} KCl, pH 7.4) for 20 min. The blocked section was incubated with the anti-PiT1-like antibody, which had been diluted to 2.5 μg ml^{-1} in Signal Enhancer HIKARI Solution A (Nacalai Tesque), for 1 h in a humid chamber. It was then incubated for another 1 h at 37°C with the fluorochrome-coupled goat anti-rabbit gamma globulin (Alexa Fluor 488; Life Technologies Corporation) diluted to 2.5 μg ml^{-1} in Signal Enhancer HIKARI Solution B (Nacalai Tesque). The slide was washed again with TPBS, counter-stained with fluorescing DNA stain, 4′ 6-diamidino-2-phenylindole (DAPI) and mounted in Prolong Gold antifade reagent (Thermo Fisher Scientific Inc.).

Digital photos were taken using an Olympus DP73 camera (Olympus Corporation, Tokyo, Japan) fitted to an Olympus BX60 epifluorescence microscope equipped with a differential interference contrast (DIC) slider (Olympus U-DICT), as well as corresponding filter sets (Olympus U-MWU, U-MWIG, and U-MNIBA) and various objectives. DIC images were taken to visualize tissue structure. For the ctenidium and the outer mantle, nuclei were stained with DAPI (in blue) and visualized using the U-MWU filter (emission at 420 nm). Autofluorescence (in red) of the plastid of symbiotic dinoflagellates in the outer mantle was captured using the U-MWIG band pass filter (emission at 580 nm). PiT1-like immunostaining (in green) was visualized using the U-MNIBA band pass filter (emission at 515–550 nm). All images were processed using the cellSens Standard v1.15 software (Olympus Corporation) and prepared using the Adobe Photoshop CS6 (Adobe Systems, CA, United States). The overlaid of images was performed using Adobe Photoshop CC.

[2]http://web.expasy.org/translate/

Statistical Analysis

Results were presented as mean + SEM. Statistical analysis was performed using SPSS Statistics version 19 software (IBM Corporation, Armonk, NY, United States). Levene's test was used to examine the homogeneity of variance among the means. Depending on the homogeneity of variances, one-way analysis of variance (ANOVA), followed by Dunnett T3 *post hoc* test or Tukey *post hoc* test, was used to evaluate differences among means. Differences among means with a p-value less than 0.05 were regarded as statistically significant.

RESULTS

Nucleotide and Deduced Amino Acid Sequences

The complete cDNA coding sequence of *PiT1-like* obtained from the kidney of *T. squamosa* (GenBank accession number MN256447) comprised 1,665 bp, and the deduced amino acid sequence had 553 amino acids with an estimated molecular mass of 59.3 kDa.

An analysis of sequence similarities among PiT1-like of *T. squamosa* and PiT1 proteins of various species obtained from GenBank (**Table 1**) indicated that it had the highest sequence similarity with those of mollusks (50.8–54.4%), followed by those of cnidarians, brachiopods and echinoderms (38.4–48.6%), and it had the lowest sequence similarity with those of plants and chlorophytes (8.8–14.3%). The host origin of PiT1-like of *T. squamosa* was validated by phenogramic analysis (**Figure 1**). The low similarity of PiT1-like of *T. squamosa* with various NPT2s confirmed that it was indeed a PiT1 transport protein (**Table 1**). In addition, the N and C terminals of PiT1-like of *T. squamosa* contained the ProDom domain (Bottger and Pedersen, 2011) and the 12 amino acid-long signature sequence (Bottger and Pedersen, 2005) characteristic of the PiT family. Typical of PiT proteins, there were 11 predicted TMs in PiT1-like of *T. squamosa*. An alignment with other PiT1s (*Homo sapiens*, *Xenopus laevis*, and *Exaiptasia diaphana*) revealed the conservation of several important residues that are critical for P_i transport (D39, E66, H403, D407, E476, and S494, numbered according to PiT1-like of *T. squamosa* in **Figure 2**). Other conserved residues included those that constituted part of the substrate binding site (V77, I86, and V88) and those responsible for substrate selectivity (S78 and R82) of P_i binding (S125).

Gene Expression of PiT1-Like in Various Organs

In *T. squamos*a, *PiT1-like* was expressed strongly in the kidney and ctenidium, and moderately in the outer mantle, inner mantle, heart, and adductor muscle. It was only weakly expressed in the hepatopancreas, byssal retractor muscle, and foot muscle (**Figure 3**). Hence, efforts were focused subsequently on elucidating the possible functions of PiT1-like in the kidney, ctenidium, and outer mantle of *T. squamosa*.

Immunofluorescence Localization of PiT1-Like

The kidneys of giant clams are known to consist of nephrocytes, which are large globular cells with indistinct boundaries and little visible cytoplasmic contents (Norton and Jones, 1992). In the kidney of *T. squamosa*, PiT1-like was localized in the membrane surrounding a type of nephrocytes (**Figure 4**). In the ctenidium of *T. squamosa*, PiT1-like had a basolateral localization in the filaments and tertiary water channels (**Figure 5**). In addition,

TABLE 1 | Percentage similarity of the deduced amino acid sequence of sodium-dependent phosphate transporter protein 1 (PiT1-like) obtained from *T. squamosa* and sodium-dependent transport proteins from other species obtained from GenBank.

Classification	Species (accession number)	Protein	Similarity (%)
Mollusca	*Pomacea canaliculata* (XP_025092447.1)	Sodium-dependent phosphate transporter 1-like	54.4%
	Crassostrea gigas (EKC21620.1)	Sodium-dependent phosphate transporter 1	52.3%
	Crassostrea virginica (XP_022325213.1)	Sodium-dependent phosphate transporter 1-like	51.9%
	Mizuhopecten yessoensis (XP_021377460.1)	Sodium-dependent phosphate transporter 1-like	50.8%
Cnidaria	*Exaiptasia pallida* (XP_020903863.1)	Sodium-dependent phosphate transporter 1-like	48.6%
	Pocillopora damicornis (XP_027050156.1)	Sodium-dependent phosphate transporter 1-like	47.8%
Brachiopoda	*Lingula anatina* (XP_013385768.1)	Sodium-dependent phosphate transporter 1-like	43.1%
Echinodermata	*Acanthaster planci* (XP_022083307.1)	Sodium-dependent phosphate transporter 1-like	38.4%
Heterokonta	*Ectocarpus siliculosus* (CBJ32177.1)	PiT family phosphate transporter	27.3%
Plantae	*Morus notabilis* (EXC01477.1)	Sodium-dependent phosphate transport protein 1	14.3%
	Theobroma cacao (EOY33772.1)	Sodium-dependent phosphate transport protein 1	11.2%
	Gossypium arboreum (KHG28505.1)	Sodium-dependent phosphate transport protein 1, chloroplastic	10.7%
	Zea mays (NP_001105269.2)	Phosphate transporter protein 1	8.8%
Chlorophyta	*Auxenochlorella protothecoides* (KFM27578.1)	Sodium-dependent phosphate transport protein 1, chloroplastic	11.8%
Mollusca	*Octopus bimaculoides* (XP_014781027.1)	Sodium-dependent phosphate transport protein 2A-like	12.7%
	Aplysia californica (XP_012937515.1)	Sodium-dependent phosphate transport protein 2A-like	10.9%
	Biomphalaria glabrata (XP_013060704.1)	Sodium-dependent phosphate transport protein 2A-like	9.8%

Sequences are arranged according to decreasing similarity.

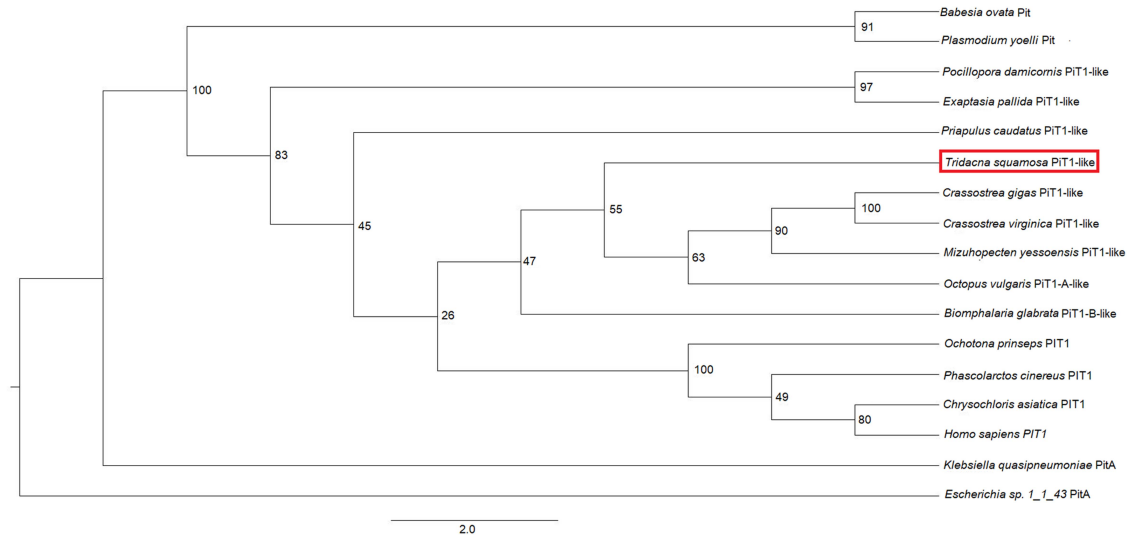

FIGURE 1 | Phenogramic analysis of the homolog of sodium-dependent phosphate transporter protein 1 (PiT1-like) from *Tridacna squamosa*. Numbers shown at each branch point represent bootstrap values from 1,500 replicates. PitA from *Escherichia sp. 1_1_43* PitA is used as the outgroup.

PiT1-like was detected in the epithelial cells of the tertiary zooxanthellal tubules in the outer mantle (**Figure 6**). In order to identify the location of PiT1-like in the tubular epithelium, it was essential to capture, albeit with some difficulties, the nuclei of the tubular epithelial cells. Nonetheless, based on three separate locations of the nuclei of the tubular epithelial cells in the image presented in **Figure 6** and many similar observations in other slide preparations, PiT1-like appeared to have a basolateral localization in the tubular epithelium.

Changes in the Transcript Levels and Protein Abundance of PiT1-Like/PiT1-Like in the Kidney, Ctenidium or Outer Mantle of *T. squamosa* in Response to Light

In *T. squamosa*, the transcript level of *PiT1-like* in the kidney was approximately 10-fold higher than those in the ctenidium and outer mantle (**Figure 7**). There were significant increases in the transcript levels of *PiT1-like* in the kidney at hour 12 of light exposure (**Figure 7A**), in the ctenidium at hour 6 or 12 of light exposure (**Figure 7B**), and in the outer mantle at hour 3 of light exposure (**Figure 7C**), when compared with the corresponding values of the control clams kept in darkness for 12 h.

As the kidney and ctenidium had apparently higher protein abundance of PiT1-like than the outer mantle, the protein loads of samples of kidney, ctenidium, and outer mantle for electrophoresis were 20, 50, and 100 μg (**Figure 8**), respectively. The protein abundance of PiT1-like increased significantly in the kidney of *T. squamosa* after 6 or 12 h of exposure to light, as compared to the control (**Figure 8A**). In comparison, the protein abundance of PiT1-like increased significantly in the ctenidium and outer mantle only after 12 h of exposure to light as compared to the control (**Figures 8B,C**). The specificity of anti-PiT1-like antibody was validated by PCA, whereby the PiT1-like band of the kidney sample was abolished using the peptide-neutralized antibody (**Supplementary Figure 1**).

DISCUSSION

Molecular Properties of PiT1-Like From *T. squamosa*

PiT1-like of *T. squamosa* consists of two homology ProDom domains (PD001131), one at the N terminal region and another at the C terminal region (Salaün et al., 2004; Bottger and Pedersen, 2011), which are characteristic of PiT proteins. Moreover, two related sequence motifs (of 12 amino acids long), which are designated as signature sequences of the PiT family and involved in cation translocation (Bottger and Pedersen, 2005), can be found in the PD001131 domains of PiT1-like of *T. squamosa*. All conserved amino acids known to be critical for P_i transport are located inside the two PD001131 domains of PiT1-like. Based on the characterization of human PiT2 (Bottger and Pedersen, 2011), residues D39, E66, H403, D407, E476, and S494 in PiT1-like of *T. squamosa* could be involved in the translocation of $H_2PO_4^-$ (Bottger and Pedersen, 2002, 2005, 2011), although the exact mechanism remains elusive (Beck et al., 2009). The two conserved glutamate residues situated in the TMs could act to couple Na^+ transport with P_i uptake (Bottger et al., 2006). Similar to PiT1 of *H. sapiens* and *X. laevis*, PiT1-like of *T. squamosa* comprises several conserved residues, such as V77, S78, R82, I86, V88, and S125, which constitute the substrate binding site(s) (Ravera et al., 2013; Bon et al., 2017). In particular, S125 may be responsible for binding of $H_2PO_4^-$ (Bon et al., 2017) while S78 and R82 are responsible for substrate selectivity and coordination (Ravera et al., 2013). As V77, S78, R82, I86, and V88 are located

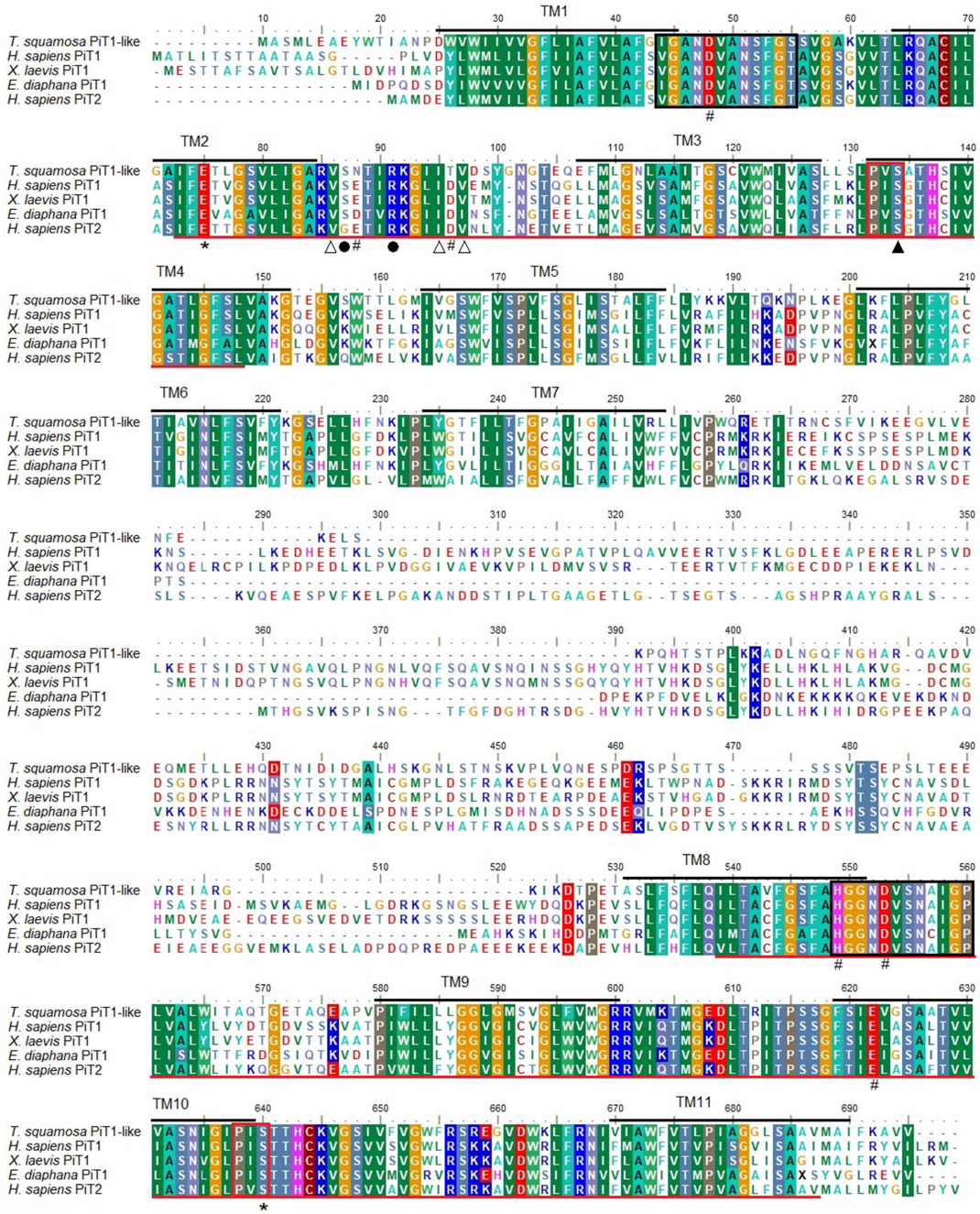

FIGURE 2 | A multiple sequence alignment of the deduced amino acid sequence of sodium-dependent phosphate transporter protein 1-homolog (PiT1-like) obtained from *Tridacna squamosa*, *Homo sapiens* PiT1 (NP_005406.3), *Xenopus laevis* PiT1 (NP_001087494.1), *Exaiptasia diaphana* PiT1 (XP_020903863.1) and the PiT2 paralog from *Homo sapiens* (Q08357.1). The 11 transmembrane regions (TMs) predicted using the TOPCONS server have been delineated in black with the region number above. The two ProDom (PD001131) domains are underlined in red. The 12 amino acid-long signature sequence of the PiT family is marked with a black box. The red boxes denote the conserved P-X-S motif at the N and C terminal (where X is a hydrophobic amino acid). Residues identified as critical for P_i transport in human PiT1 protein are indicated with asterisks while residues that are important for P_i transport in human PiT2 paralog are marked with hash. Residues marked by open triangles constitute part of the substrate binding site(s) whereas the residue marked by a closed triangle binds P_i. Residues indicated with closed circles play a role in substrate selectivity and coordination.

in the extracellular loop region 2, they may be involved in the formation of a hydrophilic pore through which substrates might interact with the binding sites during the transport cycle (Ravera et al., 2013). With conserved substrate binding sites, PiT1-like of *T. squamosa* can co-transport Na^+ and $H_2PO_4^-$ against the uphill $H_2PO_4^-$ electrochemical gradient at the

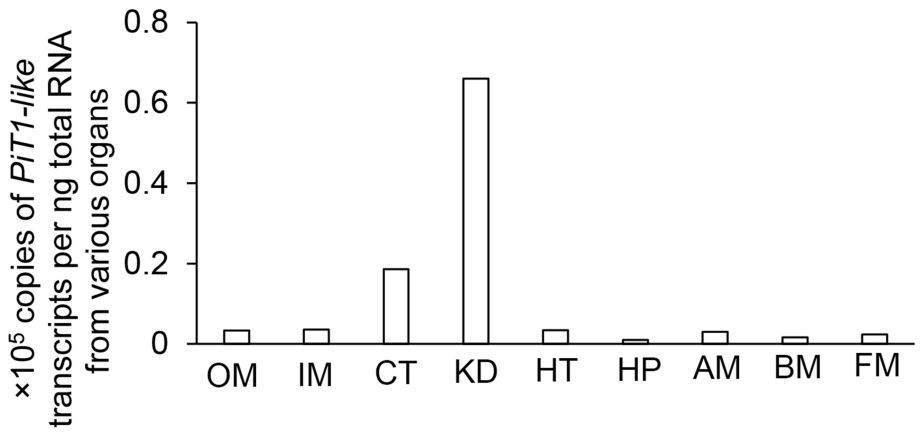

FIGURE 3 | Gene expression of a homolog of *sodium-dependent phosphate transporter protein 1* (*PiT1-like*) in the outer mantle (OM), inner mantle (IM), ctenidium (CT), kidney (KD), heart (HT), hepatopancreas (HP), adductor muscle (AM), byssal retractor muscle (BM), and foot muscle (FM) of *Tridacna squamosa* exposed to light for 12 h.

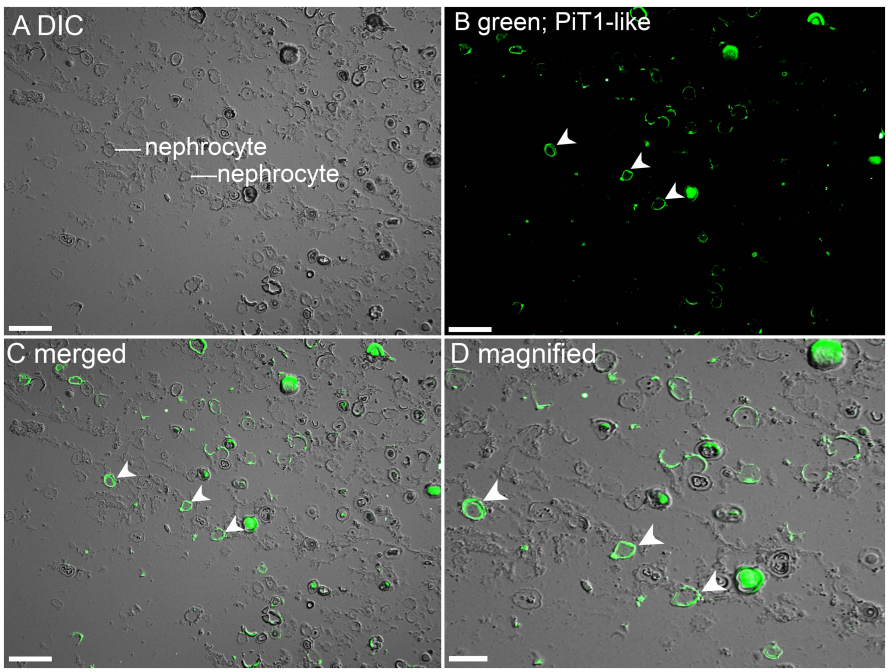

FIGURE 4 | Immunofluorescence localization of a homolog of sodium-dependent phosphate transporter protein 1 (PiT1-like) in the kidney of *Tridacna squamosa* exposed to 12 h of light. **(A)** Differential interference contrast (DIC) image to demonstrate the histological structure of kidney nephrocytes. **(B)** Green immunofluorescence staining of the membrane of kidney nephrocytes (labeled with arrowheads) indicates presence of PiT1-like protein. **(C)** Merged images of DIC with PiT1-like labeling with **(D)** a magnified view. Scale bar: **(A–C)**, 50 μm; **(D)**, 20 μm.

expense of the downhill electrochemical gradient of Na^+ through the plasma membrane into the cell.

Gene Expression of PiT1-Like in Various Organs and Its Implications

PiT1-like expression was detected in many organs of *T. squamosa*, indicating a possible house-keeping role in P_i homeostasis. However, *PiT1-like* was expressed strongly in the kidney of *T. squamosa*, which is known to contain much more phosphate than other organs (Belda and Yellowlees, 1995), denoting a probable role in the uptake and accumulation of P_i. The strong expression of *PiT1-like* in the ctenidium denotes an important physiological function, but whether it could be involved in exogenous P_i absorption depends on its subcellular localization. Furthermore, the moderate gene expression level of *PiT1-like* in the colorful outer mantle suggests an important role in the supply of P_i to the dinoflagellates

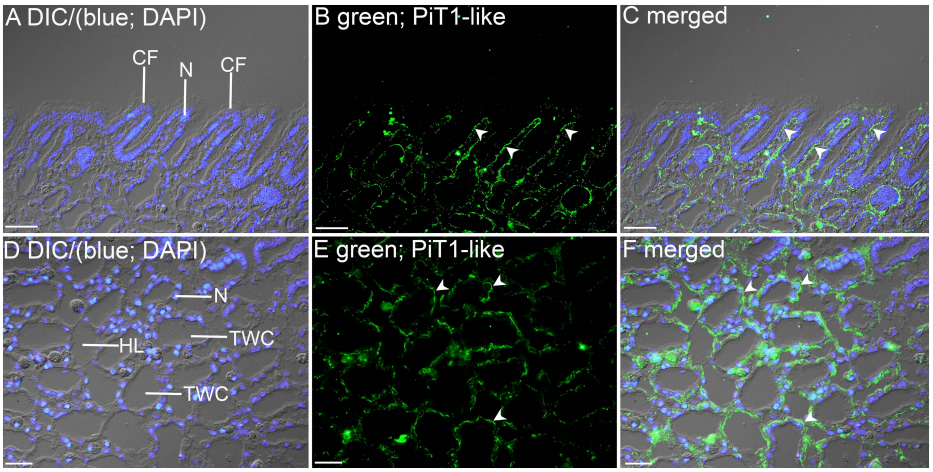

FIGURE 5 | Immunofluorescence localization of a homolog of sodium-dependent phosphate transporter protein 1 (PiT1-like) in the filament **(A–C)** or the tertiary water channels **(D–F)** in the ctenidium of *Tridacna squamosa* exposed to 12 h of light. **(A,D)** Differential interference contrast (DIC) image is overlaid with DAPI nucleus (N) stain in blue to demonstrate the histological structure of ctenidium filament (CF) and tertiary water channel (TWC). **(B,E)** PiT1-like-immunofluorescence is displayed in green. **(C,F)** The green and blue channels are overlaid with DIC. Arrowheads in **(B,C)** show extensive basolateral staining of PiT1-like on the epithelium (EP) of CFs. **(E,F)** indicates the presence of PiT1-like on the basolateral membrane of the tertiary water channels. HL, hemolymph. Scale bar: 20 μm.

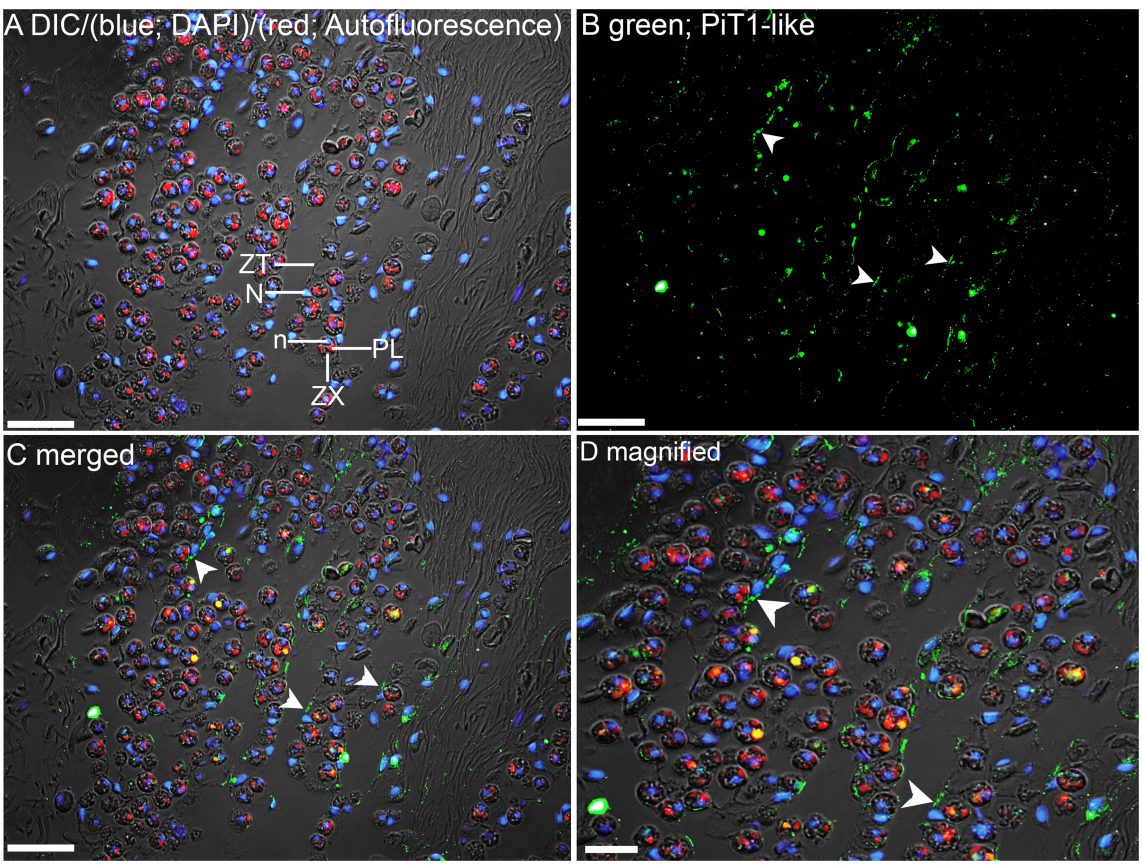

FIGURE 6 | Immunofluorescence localization of a homolog of sodium-dependent phosphate transporter protein 1 (PiT1-like) in the outer mantle of *Tridacna squamosa* exposed to 12 h of light. **(A)** Overlaid image of differential interference contrast (DIC), auto-fluorescence of symbiotic dinoflagellates (zooxanthellae, ZX) in red, merged with that of DAPI (blue) staining of zooxanthellal nucleus (n) and nucleus (N) of host tubular epithelium (ZT). Red auto-fluorescence of ZX was due to plastid (PL). **(B)** Green immunofluorescence staining of the epithelial cell linings of the basolateral membrane of ZT (labeled with arrowheads) indicates presence of PiT1-like protein. **(C)** Merged images of DIC, DAPI, red, and PiT1-like immunolabeling. **(D)** Magnified view of **(C)**. Scale bar: 20 μm.

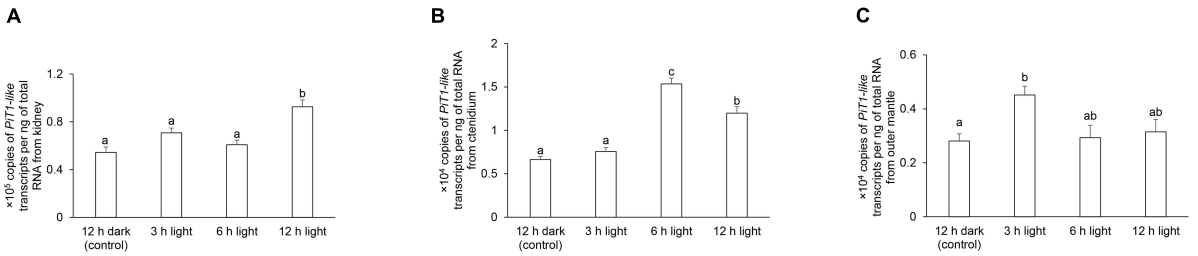

FIGURE 7 | Transcript levels of a homolog of *sodium-dependent phosphate transporter protein 1* (*PiT1-like*) from the **(A)** kidney, **(B)** ctenidium, and **(C)** outer mantle of *Tridacna squamosa* kept in darkness for 12 h (control), or exposed to light for 3, 6, or 12 h. Transcript levels of *PiT1-like* expressed as $\times 10^5$ copies of transcript per ng total RNA for kidney, or $\times 10^4$ copies of transcript per ng total RNA for ctenidium and outer mantle. Results represent means + SEM ($n = 4$). Means not sharing the same letter are significantly different (p-value < 0.05).

that are found in high density therein. In order to elucidate the functions of *PiT1-like*, it was essential to determine its cellular and subcellular localization in these three organs by immunofluorescence microscopy.

PiT1 Could Be Involved in P_i Sensing and Signaling

Extracellular P_i can act as a signaling molecule that directly alters gene expression and cellular physiology. Cells can detect changes in extracellular P_i levels through a P_i-sensing mechanism (Camalier et al., 2013; Michigami, 2013) that may involve the MAPK ERK1/2 pathway (Khoshniat et al., 2011). In human skeletal cells, PiT1 and PiT2 heterodimerization can mediate P_i signaling independent of P_i uptake (Bon et al., 2017). The deletion of PiT1 or PiT2 impedes phosphorylation mediated by the P_i-dependent MAPK ERK1/2 signaling (Bon et al., 2017). If P_iT1-like has an apical localization in epithelial cells in *T. squamosa*, it could not be involved in sensing the concentration of P_i in the hemolymph. However, if it has a basolateral localization in epithelial cells and direct contact with the hemolymph, it could possibly function as a transporter to translocate $H_2PO_4^-$ from the hemolymph into the cell, as well as a sensing mechanism to detect hemolymph $H_2PO_4^-$ but without transporting it. Although it would be difficult to decipher these two functions of P_iT1-like in *T. squamosa*, attempts were made to interpret our results based on the physiological functions of the three organs studied.

PiT1-Like Is the Light-Dependent Mechanism of P_i Uptake in Nephrocytes of the Kidney

Symbiotic animals absorb P_i from the ambient seawater not only for their own metabolism, but also for the needs of the symbionts (Jackson and Yellowlees, 1990). P_i uptake in corals (Jackson and Yellowlees, 1990; Godinot et al., 2009) and giant clams (Chan et al., 2020) are light-dependent. For giant clams, it has been postulated that the host could maintain low concentrations of P_i (<0.1 μM) in the hemolymph to control the internal population of symbiotic dinoflagellates (Belda and Yellowlees, 1995). Without knowledge of the mechanism involved, Belda and Yellowlees (1995) proposed that the kidney of giant clams could rapidly take up P_i circulating in the hemolymph to limit the availability of P_i to the symbionts. Our results demonstrate for the first time that the plasma membrane of the globular nephrocytes in the kidney of *T. squamosa* displayed a strong immunolabeling of PiT1-like. Nephrocytes are located adjacent to the hemolymph sinuses. Hence, they can probably sense the extracellular P_i concentration and actively absorb $H_2PO_4^-$ from the hemolymph through PiT1-like, driven by the electrochemical potential gradient of Na^+ (Virkki et al., 2007). Furthermore, the gene and protein expression levels of PiT1-like increased significantly in the kidney of *T. squamosa* during illumination, indicating its involvement in the increased removal of P_i from the hemolymph during light-enhanced P_i uptake to maintain a low hemolymph P_i concentration. As P_i is scarce in seawater, the host probably accumulates P_i in nephrocytes to cater for its long-term growth and development, but whether the accumulation of P_i in nephrocytes is meant to control the populations of symbionts (Belda and Yellowlees, 1995) is debatable. Results obtained from the outer mantle of *T. squamosa* indicate that the host clam could probably increase the supply of P_i to the symbionts through PiT1-like during illumination, as they would logically have a higher demand for P_i in light than in darkness.

The Basolateral PiT1-Like of the Ctenidium Probably Functions in P_i Sensing

The ctenidium of *T. squamosa* expresses NPT2a-like in the apical membrane of its epithelial cells (Chan et al., 2020). The inwardly directed Na^+ electrochemical gradient would drive HPO_4^{2-} from the ambient seawater into the epithelial cells through the apical NPT2a-like. Then, P_i can be translocated through some unknown basolateral transporter to the hemolymph. Our results indicate that the ctenidial epithelial cells of *T. squamosa* also expressed PiT1-like in the basolateral membrane. The basolateral localization prescribes that PiT1-like would transport $H_2PO_4^-$ from the hemolymph into the epithelial cells. Enterocytes of human intestine also express an apical NPT2b as well as basolateral PiT1 and PiT2 (Kiela and Ghishan, 2018), whereby NPT2b absorbs P_i from the intestinal lumen under normal circumstances, and PiT1/PiT2 function to import P_i from the blood for cellular P_i homeostasis during periods of dietary

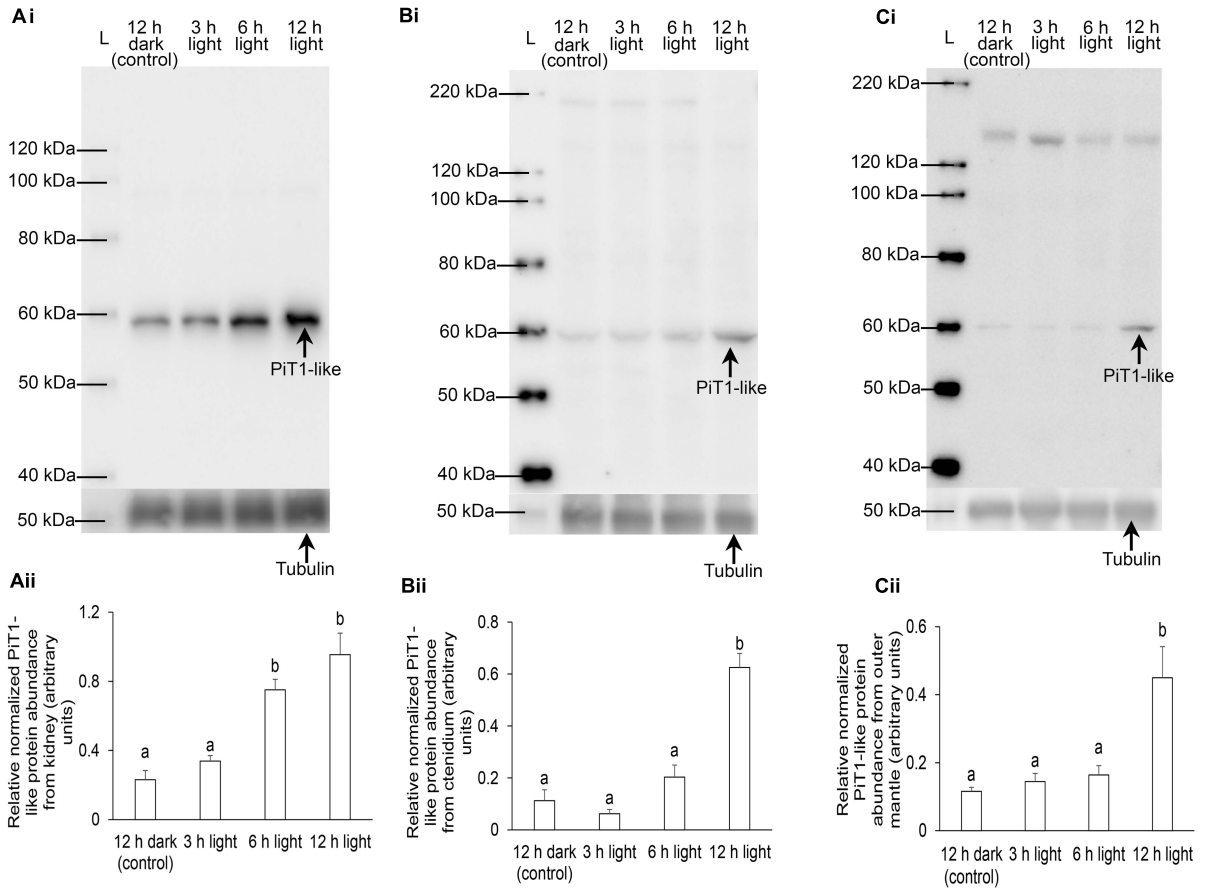

FIGURE 8 | Protein abundance of a homolog of sodium-dependent phosphate transporter protein 1 from the **(A)** kidney, **(B)** ctenidium, and **(C)** outer mantle of *Tridacna squamosa* kept in darkness for 12 h (control) or exposed to light for 3, 6, or 12 h. (i) A representative blot. L represents ladder. (ii) The optical density of the PiT1-like band for 20, 50, and 100 μg of protein from kidney, ctenidium, and outer mantle, respectively, was expressed as arbitrary units and normalized with respect to that of tubulin from each tissue. Results represent means + SEM (n = 4). Means not sharing the same letter are significantly different (p-value < 0.05).

insufficiency (Kiela and Ghishan, 2018). Hence, the possibility of the basolateral P_iT1-like in the ctenidial epithelial cells of *T. squamosa* absorbing P_i from the hemolymph during P_i-limiting situation cannot be ignored. However, the light-enhanced expression of P_iT1-like in the ctenidial epithelial cells might suggest that the capacity for P_i-sensing in these cells is enhanced by light. As P_i binding rather than P_i uptake is the key factor in mediating P_i signaling through the PiT protein, it is possible that the basolateral P_iT1-like in the ctenidial epithelial cells could act as part of a P_i-sensing mechanism, and that the physiological activities of these epithelial cells, including P_i uptake, can be regulated by the P_i concentration in the hemolymph, although future works are needed to verify these propositions.

In the Outer Mantle, PiT1-Like Could Be Involved in the Supply of P_i to the Symbionts

The outer mantle of *T. squamosa* can be regarded as a crucial site of light-enhanced P_i absorption through NPT2a-like (Chan et al., 2020), and the P_i absorbed can be delivered directly to the dinoflagellates therein. As PiT1-like had a basolateral localization in the epithelial cells that formed the tertiary tubules in the outer mantle of *T. squamosa*, it could act as a mechanism for P_i sensing and signaling. It could also actively transport $H_2PO_4^-$ from the hemolymph into the tubular epithelial cells against its concentration gradient, and then P_i could be transported through some unknown apical transporter into the luminal fluid of the zooxanthellal tubules. It has been postulated previously that the growth and reproduction of symbionts are determined by the low concentration of P_i in the hemolymph (Belda and Yellowlees, 1995). However, symbiotic dinoflagellates are surrounded by the luminal fluid of the zooxanthellal tubules, and the ionic concentrations in the luminal fluid are most likely different from those in the hemolymph. In fact, PiT1-like could logically facilitate and regulate the translocation of P_i from the hemolymph into the luminal fluid surrounding the symbionts.

Importantly, the transcript level and protein abundance of *PiT1-like*/PiT1-like increased significantly in the outer mantle at hour 3 and hour 12 of light exposure, respectively. The increase in the protein abundance of PiT1-like in the outer mantle occurred

between hour 6 and hour 12, which aligned well with the light–enhanced expression of RuBisCO protein therein (Poo et al., 2020), and with the light-enhanced host's carbon concentration mechanism (Ip et al., 2017, 2018). In light, photosynthesizing dinoflagellates need P_i to increase the synthesis of ATP during the light-dependent process of photosynthesis. The localization and light-dependency of PiT1-like expression in the outer mantle provide novel insights into the interaction between the host clam and the symbionts.

CONCLUSION

Results obtained from this study have three implications. Firstly, the same host transporter (PiT1-like) could serve different physiological functions in different organs (kidney, ctenidium, and outer mantle). Secondly, the host could probably regulate the supply of P_i to the symbionts through PiT1-like of the tubular epithelial cells. Thirdly, the increase in the supply of P_i to the symbionts, together with the absorption of P_i by nephrocytes, led to the low concentration of P_i in the hemolymph. When taken together, these results denote that the accumulation of P_i in the kidney of giant clams is unlikely to be dedicated for the control of the internal dinoflagellate population, but to act as a P_i reserve for the host's growth and development due to the scarcity of P_i in the environment.

DATA AVAILABILITY STATEMENT

The datasets presented in this study can be found in online repositories. The names of the repository/repositories and accession number(s) can be found in the article/ **Supplementary Material**.

ETHICS STATEMENT

Institutional (National University of Singapore Institutional Animal Care and Use Committee) approval was not required for research on invertebrates including giant clams. Nonetheless, giant clams were anesthetized with 0.2% phenoxyethanol before tissue sample collection.

AUTHOR CONTRIBUTIONS

YI and SC: conceptualization, writing – original draft preparation, and supervision. YI: methodology and funding acquisition. YI, MB, JP, and SC: formal analysis and investigation and writing – review and editing. WW: resources. All authors contributed to the article and approved the submitted version.

FUNDING

This study was supported by the Singapore Ministry of Education through a grant to YI (R-154-000-B69-114).

SUPPLEMENTARY MATERIAL

The Supplementary Material for this article can be found online at: https://www.frontiersin.org/articles/10.3389/fmars.2021.655714/full#supplementary-material

Supplementary Figure 1 | Peptide competition assay (PCA) on anti-PiT1-like antibody. The presence of PiT1-like band of a kidney sample exposed to light for 12 h **(A)** disappeared when anti-PiT1-like antibody was neutralized with the immunizing peptide **(B)**. L, ladder.

REFERENCES

Addessi, L. (2001). Giant clam bleaching in the lagoon of takapoto atoll (french polynesia). *Coral Reefs* 19:220.

Beck, L., Leroy, C., Salaun, C., Margall-Ducos, G., Desduoets, C., and Friedlander, G. (2009). Identification of a novel function of PiT1 critical for cell proliferation and independent of its phosphate transport activity. *J. Biol. Chem.* 284, 31363–31374. doi: 10.1074/jbc.M109.053132

Belda, C. A., and Yellowlees, D. (1995). Phosphate acquisition in the giant clam-zooxanthellae symbiosis. *Mar. Biol.* 124, 261–266.

Bon, N., Couasnay, G., Bourgine, A., Sourice, S., Beck-Cormier, S., Guicheux, J., et al. (2017). Phosphate (Pi)-regulated heterodimerization of the high-affinity sodium-dependent Pi transporters PiT1/Slc20a1 and PiT2/Slc20a2 underlies extracellular Pi sensing independently of Pi uptake. *J. Biol. Chem.* 293, 2102–2114. doi: 10.1074/jbc.M117.807339

Bottger, P., Hede, S. E., Grunnet, M., Høyer, B., Klærke, D. A., and Pedersen, L. (2006). Characterization of transport mechanisms and determinants critical for Na^+-dependent P_i symport of the PiT family paralogs human PiT1 and PiT2. *Am. J. Physiol. Cell. Physiol.* 291, 1377–1387. doi: 10.1152/ajpcell.00015.2006

Bottger, P., and Pedersen, L. (2002). Two highly conserved glutamate residues critical for type III sodium-dependent phosphate transport revealed by uncoupling transport function from retroviral receptor function. *J. Biol. Chem.* 277, 42741–42747. doi: 10.1074/jbc.M207096200

Bottger, P., and Pedersen, L. (2011). Mapping of the minimal inorganic phosphate transporting unit of human PiT2 suggests a structure universal to PiT-related proteins from all kingdoms of life. *BMC Biochem.* 12:21. doi: 10.1186/1471-2091-12-21

Bottger, P., and Pedersen, L. (2005). Evolutionary and experimental analyses of inorganic phosphate transporter PiT family reveals two related signature sequences harboring highly conserved aspartic acids critical for sodium-dependent phosphate transport function of human PiT2. *FEBS J.* 272, 3060–3074. doi: 10.1111/j.1742-4658.2005.04720.x

Camalier, C. E., Yi, M., Yu, L. R., Hood, B. L., Conrads, K. A., Lee, Y. J., et al. (2013). An integrated understanding of the physiological response to elevated extracellular phosphate. *J. Cell. Physiol.* 228, 1536–1550.

Chan, C. Y. L., Hiong, K. C., Boo, M. V., Choo, C. Y. L., Wong, W. P., Chew, S. F., et al. (2018). Light exposure enhances urea absorption in the fluted giant clam *Tridacna squamosa* and up-regulates the protein abundance of a light-dependent urea active transporter DUR3-like in its ctenidium. *J. Exp. Biol.* 221:jeb176313. doi: 10.1242/jeb.176313

Chan, C. Y. L., Hiong, K. C., Choo, C. Y. L., Boo, M. V., Wong, W. P., Chew, S. F., et al. (2019). Increased apical sodium-dependent glucose transporter abundance in the ctenidium of the giant clam *Tridacna squamosa* upon illumination. *J. Exp. Biol.* 222:jeb195644. doi: 10.1242/jeb.195644

Chan, C. Y. L., Hiong, K. C., Choo, C. Y. L., Boo, M. V., Wong, W. P., Chew, S. F., et al. (2020). Light-enhanced phosphate absorption in the fluted giant clam, *Tridacna squamosa*, entails an increase in the expression of sodium-dependent phosphate transporter 2a in its colourful outer mantle. *Coral Reefs* 39, 1055–1070. doi: 10.1007/s00338-020-01930-w

Chew, S. F., Koh, C. Z. Y., Hiong, K. C., Choo, C. Y. L., Wong, W. P., Neo, M. L., et al. (2019). Light-enhanced expression of carbonic anhydrase 4-like supports shell formation in the fluted giant clam *Tridacna squamosa*. *Gene* 683, 101–112. doi: 10.1016/j.gene.2018.10.023

DeBoer, T. S., Baker, A. C., Erdmann, M. V., Ambariyanto, Jones, P. R., and Barber, P. H. (2012). Patterns of *Symbiodinidium* distribution in three giant clam species across the biodiverse bird's head region of indonesia. *Mar. Ecol. Prog. Ser.* 444, 117–132. doi: 10.3354/meps09413

Fitt, W. K., and Trench, R. K. (1981). Spawning, development and acquisition of zooxanthellae by *Tridacna squamosa* (mollusca, bivalvia). *Biol. Bull.* 161, 213–235. doi: 10.2307/1540800

Forster, I. C., Hernando, N., Biber, J., and Murer, H. (2013). Phosphate transporters of the SLC20 and SLC34 families. *Mol. Aspects Med.* 34, 386–395. doi: 10.1016/j.mam.2012.07.007

Furla, P., Allemand, D., Shick, J. M., Ferrier-Pagès, C., Richier, S., Plantivaux, A., et al. (2005). The symbiotic anthozoan: a physiological chimera between alga and animal. *Integ. Comp. Biol.* 45, 595–604. doi: 10.1093/icb/45.4.595

Godinot, C., Ferrier-Pages, C., and Grover, R. (2009). Control of phosphate uptake by zooxanthellae and host cells in the scleractinian coral stylophora pistillata. *Limnol. Oceanogr.* 54, 1627–1633. doi: 10.4319/lo.2009.54.5.1627

Hernawan, U. E. (2008). Review: symbiosis between the giant clams (bivalvia: cardiidae) and zooxanthellae (dinophyceae). *Jurusan Biol.* 9, 53–58. doi: 10.13057/biodiv/d090113

Hiong, K. C., Cao-Pham, A. H., Choo, C. Y. L., Boo, M. V., Wong, W. P., Chew, S. F., et al. (2017a). Light-dependent expression of a Na^+/H^+ exchanger 3-like transporter in the ctenidium of the giant clam, *Tridacna squamosa*, can be related to increased H^+ excretion during light-enhanced calcification. *Physiol. Rep.* 5:e13209. doi: 10.14814/phy2.13209

Hiong, K. C., Choo, C. Y. L., Boo, M. V., Ching, B., Wong, W. P., Chew, S. F., et al. (2017b). A light-dependent ammonia-assimilating mechanism in the ctenidia of a giant clam. *Coral Reefs* 36, 311–323.

Ikeda, S., Yamashita, H., Kondo, S., Inoue, K., Morishima, S., and Koike, K. (2017). Zooxanthellal genetic varieties in giant clams are partially determined by species-intrinsic and growth-related characteristics. *PLoS One* 12:e0172285. doi: 10.1371/journal.pone.0172285

Ip, Y. K., and Chew, S. F. (2021). Light-dependent phenomena and related molecular mechanisms in giant clam-dinoflagellate associations: a review. *Front. Mar. Sci.* 8:627722. doi: 10.3389/fmars.2021.627722

Ip, Y. K., Ching, B., Hiong, K. C., Choo, C. Y. L., Boo, M. V., Wong, W. P., et al. (2015). Light induces changes in activities of Na^+/K^+-ATPase, H^+/K^+-ATPase and glutamine synthetase in tissues involved directly or indirectly in light-enhanced calcification in the giant clam, *Tridacna squamosa*. *Front. Physiol.* 6:68. doi: 10.3389/fphys.2015.00068

Ip, Y. K., Hiong, K. C., Lim, L. J. Y., Choo, C. Y. L., Boo, M. V., Wong, W. P., et al. (2018). Molecular characterization light-dependent expression and cellular localization of a host vacuolar-type H^+-ATPase (VHA) subunit A in the giant clam *Tridacna squamosa* indicate the involvement of the host VHA in the uptake of inorganic carbon and its supply to the symbiotic zooxanthellae. *Gene* 659, 137–148. doi: 10.1016/j.gene.2018.03.054

Ip, Y. K., Hiong, K. C., Teng, J. H. Q., Boo, M. V., Choo, C. Y. L., Wong, W. P., et al. (2020). The fluted giant clam (*Tridacna squamosa*) increases nitrate absorption and upregulates the expression of a homolog of SIALIN (H^+:$2NO_3^-$ cotransporter) in the ctenidium during light exposure. *Coral Reefs* 39, 451–465. doi: 10.1007/s00338-020-01907-9

Ip, Y. K., Koh, C. Z. Y., Hiong, K. C., Choo, C. Y. L., Boo, M. V., Wong, W. P., et al. (2017). Carbonic anhydrase 2-like in the giant clam, *Tridacna squamosa*: characterization, localization, response to light, and possible role in the transport of inorganic carbon from the host to its symbiont. *Physiol. Rep.* 5:e13494. doi: 10.14814/phy2.13494

Ip, Y. K., Loong, A. M., Hiong, K. C., Wong, W. P., Chew, S. F., Reddy, K., et al. (2006). Light induces an increase in the pH of, and a decrease in the ammonia concentration in, the extrapallial fluid of the giant clam *Tridacna squamosa*. *Physiol. Biochem. Zool.* 79, 656–664.

Jackson, A. E., Miller, D. J., and Yellowlees, D. (1989). Phosphorus metabolism in the coral-zooxanthellae symbiosis: characterization and possible roles of two acid phosphatases in the algal symbiont *Symbiodinium* sp. *Proc. R. Soc. Lond. B* 238, 193–202. doi: 10.1098/rspb.1989.0076

Jackson, A. E., and Yellowlees, D. (1990). Phosphate uptake by zooxanthellae isolated from corals. *Proc. R. Soc. Lond. B* 242, 204–210. doi: 10.1098/rspb.1989.0076

Khoshniat, S., Bourgine, A., Julien, M., Petit, M., Pilet, P., Rouillon, T., et al. (2011). Phosphate-dependent stimulation of MGP and OPN expression in osteoblasts via the ERK1/2 pathway is modulated by calcium. *Bone* 48, 894–902.

Kiela, P. R., and Ghishan, F. K. (2018). *Chapter 59 Molecular mechanisms of intestinal transport of calcium, phosphate and magnesium. In Physiology of Gastrointestinal Tract*, Sixth Edn. Amsterdam: Elsevier Inc, 1405–1449.

Klumpp, D. W., and Griffiths, C. L. (1994). Contributions of phototrophic and heterotrophic nutrition to the metabolic and growth requirements of four species of giant clam (tridacnidae). *Mar. Ecol. Progr. Ser.* 115, 103–115. doi: 10.3354/meps115103

Knowles, J. R. (1980). Enzyme-catalyzed phosphoryl transfer reactions. *Ann. Rev. Biochem.* 49, 877–919. doi: 10.1146/annurev.bi.49.070180.004305

Koh, C. Z. Y., Hiong, K. C., Choo, C. Y. L., Boo, M. V., Wong, W. P., Chew, S. F., et al. (2018). Molecular characterization of a dual domain carbonic anhydrase from the ctenidium of the giant clam, *Tridacna squamosa*, and its expression levels after light exposure, cellular localization, and possible role in the uptake of exogenous inorganic carbon. *Front. Physiol.* 9:281. doi: 10.3389/fphys.2018.00281

LaJeunesse, T. C., Parkinson, J. E., Gabrielson, P. W., Jeong, H. J., Reimer, J. D., Voolstra, C. R., et al. (2018). Systematic revision of symbiodiniaceae highlights the antiquity and diversity of coral endosymbionts. *Curr. Biol.* 28, 2570–2580. doi: 10.1016/j.cub.2018.07.008

Lim, S. S. Q., Huang, D., Soong, K., and Neo, M. L. (2019). Diversity of endosymbiotic symbiodiniaceae in giant clams at dongsha atoll, northern south china sea. *Symbiosis* 78, 251–262. doi: 10.1007/s13199-019-00615-5

Michigami, T. (2013). Extracellular phosphate as a signaling molecule. *Contrib. Nephrol.* 180, 14–24.

Norton, J. H., and Jones, G. W. (1992). *The giant clam: an anatomical and histological atlas*. Canberra Australia: Australian Centre for International Agricultural Research.

Olsen, J. V., Blagoev, B., Gnad, F., Macek, B., Kumar, C., Mortensen, P., et al. (2006). Global, in vivo, and site-specific phosphorylation dynamics in signaling networks. *Cell* 127, 635–648. doi: 10.1016/j.cell.2006.09.026

Poo, J. S. T., Choo, C. Y. L., Hiong, K. C., Boo, M. V., Wong, W. P., Chew, S. F., et al. (2020). Phototrophic potential and form II ribulose-1,5-bisphosphate carboxylase/oxygenase expression in five organs of the fluted giant clam, *Tridacna squamosa*. *Coral Reefs* 39, 361–374. doi: 10.1007/s00338-020-01898-7

Ravera, S., Murer, H., and Forster, I. C. (2013). An externally accessible linker region in the sodium-coupled phosphate transporter PiT-1 (SLC20A1) is important for transport function. *Cell. Phys. Biochem.* 32, 187–199. doi: 10.1159/000350135

Rivkin, R. B., and Swift, E. (1985). Phosphorus metabolism of oceanic dinoflagellates: phosphate uptake, chemical composition and growth of *Pyrocystis noctiluca*. *Mar. Biol.* 88, 189–198. doi: 10.1007/BF00397166

Salaün, C., Maréchal, V., and Heard, J. M. (2004). Transport-deficient Pit2 phosphate transporters still modify cell surface oligomers structure in response to inorganic phosphate. *J. Mol. Biol.* 340, 39–47. doi: 10.1016/j.jmb.2004.04.050

Virkki, L. V., Biber, J., Murer, H., and Forster, I. C. (2007). Phosphate transporters: a tale of two solute carrier families. *Am. J. Physiol. Renal. Physiol.* 293, 643–654. doi: 10.1152/ajprenal.00228.2007

Watson, S. A. (2015). Giant clams and rising CO_2: Light may ameliorate effects of ocean acidification on a solar-powered animal. *PLoS One* 10:e0128405. doi: 10.1371/journal.pone.0128405

Weber, M. (2009). *The biogeography and evolution of Symbiodinium in giant clams (Tridacnidae)*. PhD thesis. Berkeley: University of California.

Conflict of Interest: The authors declare that the research was conducted in the absence of any commercial or financial relationships that could be construed as a potential conflict of interest.